Environ Earth Sci (2016) 75:51
DOI 10.1007/s12665-015-4869-6

ORIGINAL ARTICLE

Identification of dissolved sulfate sources and the role of sulfuric acid in carbonate weathering using $\delta^{13}C_{DIC}$ and $\delta^{34}S$ in karst area, northern China

Huang Qibo[1,2,3] · Qin Xiaoqun[2,3] · Yang Qiyong[2,3] · Liu Pengyu[2,3] · Zhang Jinsong[2,3]

Received: 6 December 2014 / Accepted: 28 July 2015 / Published online: 21 December 2015

Abstract Karst groundwater is one of the most important water resources for agriculture and industry in Fenyang City of Shanxi province, northern China. In the last few decades, excessive exploitation of groundwater and other human activities have caused serious environmental problems in this area. Hence, it is essential to identify the resources of pollutants that deteriorate the water quality in the area. A total of 16 water samples were collected to assess the hydrochemical characteristics from wells and springs in bare karst area, northern Fenyang and covered karst region, south of the city. The chemical composition of groundwater was characterized by a dominance of Ca^{2+}, Mg^{2+}, HCO_3^-, and SO_4^{2-}, which accounted for more than 85 % of the total ion concentrations, indicating that limestone dissolution by weathering controls water chemical composition. SO_4^{2-} in the groundwater showed high positive significant correlation with HCO_3^- and $\delta^{13}C_{DIC}$, showing that carbonate dissolution by sulfuric acid has important contribution to groundwater chemical composition and $\delta^{13}C_{DIC}$ value. The relationship between $\delta^{34}S$ and $1/SO_4^{2-}$ revealed that the sources of SO_4^{2-} are different in various types of groundwater. In the bare karst area, SO_4^{2-} in springs mainly came from atmospheric precipitation, while in the shallow wells it mainly came from human activities; in the covered karst region, SO_4^{2-} in quaternary pores water was mainly from anthropogenic inputs, while in the deep wells it was mainly from gypsum dissolution; in gypsum mine water, SO_4^{2+} was mainly from gypsum dissolution. Comparing with the bare karst area, human activities have significantly changed the chemical composition of groundwater in the covered karst region. Therefore, more control policies and measures should be formulated and applied to protect the covered karst region in the future.

Keywords Karst water · Carbon isotope · Sulfate isotope · Sulphuric acid · China

Introduction

Karst groundwater is a major water resource in karst regions, especially in population growing areas (Wang et al. 2006; Han et al. 2006). In the last few decades, the combined effects of extreme climate and intense human activities have caused groundwater depletion and deterioration in many karst areas throughout the world (Fan et al. 2013), such as France (Gams et al. 1993), the United States (Beynen et al. 2007), Serbia (Jemcov 2007), Italy (Sauro 1993), Germany (Heinz et al. 2008) and China (Guo et al. 2005). However, karst systems are known for their high vulnerability to be contaminated by surface water or wastewater due to their high hydraulic conductivities and strong surface water–groundwater interaction (Heinz et al. 2008). The karst systems are extremely difficult to recover once being damaged (Li et al. 2010a, b). In northern China, nearly 80 % of spring discharge has been declining at a rate of 1–2 m/year due to climate change and anthropogenic activities since the 1950s (Guo et al. 2005). Furthermore,

✉ Yang Qiyong
yangqiyong0739@163.com

1 School of Environmental Studies, China University of Geosciences, Wuhan 430074, China

2 Institute of Karst Geology, Chinese Academy of Geological Sciences, Guilin 541004, China

3 Karst Laboratory of Karst Dynamics, Ministry of Land and Resources/Guangxi Zhuang Autonomous Region, Guilin 541004, China

more than 20 % of the water in the main discharge zone has been deteriorated in karst water system in northern China, and the water quality was under III class (Liang et al. 2013).

Dissolved inorganic carbon (DIC) and Sulfate (SO_4^{2-}) are ubiquitous components of groundwater, derived from both natural and anthropogenic sources. Moreover, elevated SO_4^{2-} concentrations often characterize contamination in natural waters (Krouse and Mayer 2000; Spence and Telmer 2005; Otero et al. 2007). Isotope technology has been proved to be an effective method for exploring hydrogeology of groundwater systems in a karst region. Many studies on application of isotope technology have been carried out in the Southwest China karst area. Carbon isotope in DIC and Sulfate-S isotope have been used successfully to identify different pollution sources of natural and anthropogenic aquatic environments (Bottrell et al. 2008; Hosono et al. 2010; Lang et al. 2011). $\delta^{13}C_{DIC}$ and stoichiometry analyses have been applied to assessing the effect of sulfuric acid on carbonate weathering in Xijiang River (upper Pearl River), Southwest China (Li et al. 2008). The dissolved SO_4^{2-} and its $\delta^{34}S$ have been utilized to evaluate the mixing and transport processes of karst water from different sources in Southwest China (Liu et al. 2008; Zhang et al. 2009; Li et al. 2010a, b; Yang et al. 2010; Lang et al. 2011). The main objectives of this study are: (a) to assess the groundwater quality with major ion hydrochemistry; (b) to identify the sulfate sources of karst water; and, (c) to identify hydrochemical processes by carbon and sulfur isotopes in bare karst area and covered karst region in Fenyang City of Shanxi province, northern China.

Study area

Fenyang City, being bounded by latitude 37°9′26″ to 37°29′02″N and longitude 111°25′40″ to 112°00′00″E, is located in southwest Jinzhong basin, south of Luliang Mountain in Shanxi Province, northern China. It has a subtropical humid monsoon climate. The average annual temperature is 11.1 °C (max 39.9 °C; min −27.4 °C), and the annual precipitation is 444.4 mm (high 718.1 mm; low 260.7 mm), out of which 50–75 % falls in the summer (June–September).

The study area is divided into northern and southern karst water system by F3 fault (Fig. 1). The north part is a bare karst area, with an elevation of 1100–1900 m above the sea level, in which the strata are primarily carbonate rocks (limestone and dolomite) of the Cambrian-Ordovician system. The karst water is mainly supplied by precipitation and flows southward until it is blocked by Archaean metamorphic rocks and form the Mapao Spring (D10) and Xiakuo Spring (D11) (Fig. 1). Meanwhile, there are epikarst springs developed in local low-lying karst valleys and shallow wells drilled in structure zones. The south part is a covered karst region with an elevation of 1100–1300 m, where Cambrian-Ordovician carbonate rocks are buried by the middle Pleistocene loess. The karst water is recharged by precipitation and river seepage in exposed area in northeast. It migrates from northeast to southwest through artificial discharge by deep well pumping with 500–800 m depth. There are wells with high porosity and a depth of 130–180 m in Middle Pleistocene loess layer. There is a gypsum mine in the southwest of the Ordovician strata, with a spring 10 m under the gypsum mine.

Methodology

Samples and pretreatment in the field

In this study, the hydrochemistry, C isotope in DIC, and Sulfate-S isotopic compositions were analyzed in shallow wells and karst springs in northern bare karst area, in deep wells and quaternary pore water wells in southern covered karst region, and in gypsum mine water. A total of 16 locations were sampled from two Quaternary pore wells, five karst deep wells, two karst shallow wells, six karst springs and a gypsum mine on July, 2011 (Fig. 1). The parameters including water pH (±0.01 pH units), temperature ($T \pm 0.1$), and electrical conductivity (Ec ± 0.5 %) were measured in situ using the HQ340d muti-parameter meter by HACH Co. (USA). Alkalinity (counted and denoted as HCO_3^-) was titrated in the field using a portable testing kit produced by Merck KGaA Co. (Germany). Discharge was measured by YSD5 velocity measurement instrument produced by Shaanxi Xinyuan technology Company. The precision of the measurements is approximately 0.01 L/s.

All water samples were filtered through 0.45 μm pore-size membrane filters on site. Filtered water samples were stored and airproofed in three new 350 ml polyethylene (HDPE) bottles. One of them was acidified to a pH of 2.0 with distilled 1:1 HNO_3 for cation analyses, the second was preserved with $HgCl_2$ for C isotopes analyses, and the third was left untreated for the analyses of anions. For the preparation for S isotope analysis, an additional aliquot of 5 L of water was collected, and acidified with distilled HCl to pH of 2.0 to remove HCO_3^- and CO_3^{2-}. This sample was filtered later in the laboratory.

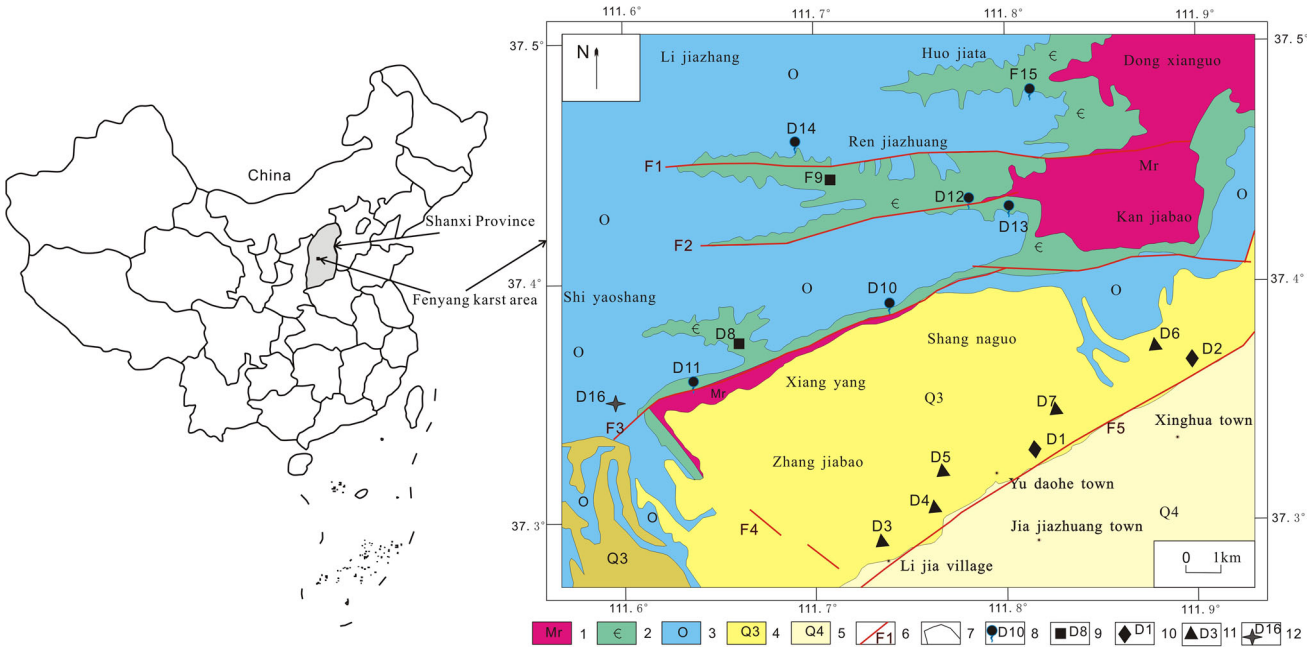

Fig. 1 Hydrogeology map of Fenyang. *1* Archaean metamorphic rock, *2* Cambrian carbonate rocks, *3* Ordovician carbonate rocks, *4* Middle Pleistocene loess layer, *5* Quaternary diluvium layer, *6* Fault and number, *7* Stratigraphic boundary, *8* Spring and number, *9* Shallow well and number, *10* Quaternary pore water well and number, *11* Spring and number, *12* Gypsum mine water and number

Analytical methods

Major anions (Cl^-, NO_3^-, SO_4^{2-}) were tested using ion chromatography and major cations (K^+, Na^+, Ca^{2+}, Mg^{2+}) were analyzed by ICP-OES (Optima.2100DV, Perkin-Elmer CO., USA) in Inspection and Supervision Centre for Resources and Environment of Karst Geology, Ministry of Land and Resources, following US Environment Protection Agency (EPA) standard methods. The charge balance of anions and cations was cross-checked and found to show a difference of <5 %.

For $\delta^{13}C$ of DIC, CO_2 was collected in an off-line vacuum system according to the method of Atekwana and Krishnamurthy (1998). The carbon isotope ratios of DIC were analyzed in Inspection and Supervision Centre for Resources and Environment of Karst Geology, Ministry of Land and Resources, using a Finnigan MAT-252 mass spectrometer and reported using the δ notation relative to Pee Dee belemnite (PDB, ‰). Routine $\delta^{13}C_{DIC}$ measurements have a precision of ±0.1 ‰.

For $\delta^{34}S$ of SO_4^{2-} analysis, 10 % $BaCl_2$ was added to the water sample to precipitate dissolved SO_4^{2-} as $BaSO_4$. The precipitation ($BaSO_4$) was collected on a 0.45 μm Millipore membrane filter and dried in an oven at 60 °C for 3 h. Sulfate isotope analyses were executed by isotope ratio mass spectrometry after converting $BaSO_4$ to SO_2 via high-temperature reaction of $BaSO_4$ with V_2O_5 and SiO_2 (Yanagisawa and Sakai 1983). The Sulfate isotope ratios of SO_2 were determined in Isotope Geochemistry Laboratory, Wuhan Institute of Geology and Mine (CAGS), using a mass spectrometer (MAT-252) and reported using the δ notation relative to the Vienna Canyon Diablo Troilite (V-CDT) standard. The precision of the measurements is approximately ±0.5 ‰, but typically ±0.2 ‰.

Results

General characteristics

The chemical compositions and isotopic ratios of groundwater samples are listed in Table 1. The pH values ranged from 7.39 to 7.89, with a mean of 7.65, signifying that alkalinity is imparted primarily due to bicarbonates, which reflects the dissolution of limestone and dolomite in the study area (Li et al. 2011). As to measure the total dissolved content, the total cation charge ($TZ^+ = K^+ + Na^+ + 2Ca^{2+} + 2\ Mg^{2+}$) varied from 4.34 to 9.98 meq/L, with a mean value of 6.03 meq/L. On the other hand, the total anion charge ($TZ^- = HCO_3^- + Cl^- + NO_3^- + 2SO_4^{2-}$) varied from 4.21 to 9.61 meq/L, with a mean value of 5.83 meq/L. There are three exceptions, namely the samples of D02, D07 and D16. Samples D02 and D07 in the southern covered karst region were polluted by waste water from human pollution, which have a high cation and anion charge (Table 1). Sample D16 for gypsum

Table 1 Major ions and sulfur, carbon isotope composition in different types of groundwater from Fenyang

No.	Type	Well deep (m)	Discharge (L/S)	T (°C)	pH	Ec (μs/cm)	K^+ (mmol/L)	Na^+	Ca^{2+}	Mg^{2+}	Cl^-	SO_4^{2-}	HCO_3^-	NO_3^-	TZ^+ (meq/L)	TZ^-	NICB (%)	SIC	PCO_2	$\delta^{34}S$ (‰)	$\delta^{13}C$
D01	Pore well	130	–	14.3	7.71	422	0.02	0.90	1.32	0.95	0.40	0.19	4.03	0.34	5.45	5.15	2.86	0.20	−2.40	11.05	−8.51
D02		180	–	16.8	7.55	586	0.06	5.61	1.17	2.48	3.04	1.96	5.53	0.43	12.97	12.93	0.14	0.14	−2.10	9.46	−7.53
D03	Deep well	700	–	24.4	7.39	970	0.08	3.16	2.18	1.20	3.51	0.87	4.22	0.14	9.98	9.61	1.91	0.20	−2.01	19.35	−9.41
D04		700	–	21.0	7.71	439	0.03	0.80	1.40	0.85	0.47	0.20	4.01	0.19	5.34	5.08	2.44	0.32	−2.36	8.73	−9.27
D05		601	–	20.0	7.60	577	0.05	0.94	1.57	1.15	0.70	0.61	4.43	0.14	6.43	6.47	−0.35	0.26	−2.22	15.69	−9.59
D06		800	–	24.5	7.53	433	0.06	0.98	1.88	1.25	0.70	1.12	4.08	0.13	7.29	7.15	1.02	0.27	−2.16	17.61	−9.53
D07		650	–	20.6	7.39	585	0.09	1.70	2.57	3.08	1.05	2.35	6.74	0.10	13.09	12.59	1.94	0.25	−1.84	9.53	−7.69
D08	Shallow well	70	–	15.9	7.56	626	0.05	0.30	2.05	1.18	0.32	0.62	4.70	0.25	6.81	6.52	2.14	0.30	−2.18	4.66	−11.7
D09		100	–	14.2	7.51	572	0.03	0.27	2.34	1.01	0.47	0.36	4.56	0.90	7.00	6.65	2.53	0.28	−2.15	4.53	−12.3
D10	Karst spring	–	320.00	13.0	7.72	393	0.02	0.22	1.74	0.70	0.20	0.13	4.25	0.11	5.11	4.81	2.96	0.34	−2.39	5.06	−10.9
D11		–	350.00	13.9	7.77	360	0.04	0.36	1.32	0.65	0.30	0.12	3.53	0.15	4.34	4.21	1.58	0.22	−2.51	6.42	−10.4
D12		–	5.57	13.4	7.86	436	0.06	0.23	1.83	0.79	0.27	0.31	4.36	0.08	5.53	5.33	1.87	0.53	−2.51	4.83	−11.5
D13		–	5.64	13.5	7.68	352	0.03	0.20	1.38	0.70	0.22	0.20	3.70	0.07	4.39	4.40	-0.10	0.21	−2.38	4.73	−9.06
D14		–	2.37	13.7	7.81	585	0.02	0.21	1.87	0.79	0.27	0.30	4.56	0.10	5.54	5.55	-0.04	0.43	−2.47	5.32	−10.9
D15		–	24.78	13.8	7.89	388	0.02	0.22	1.74	0.70	0.22	0.12	4.36	0.09	5.13	4.91	2.15	0.53	−2.55	5.57	−10.9
D16	Gypsum water	–	3.53	13.3	7.65	1546	0.07	0.42	5.56	2.33	0.42	5.62	4.43	0.19	16.27	16.28	-0.05	0.68	−2.30	19.28	−9.99

$NICB = (TZ^+ - TZ^-) \times 100/(TZ^+ + TZ^-)$

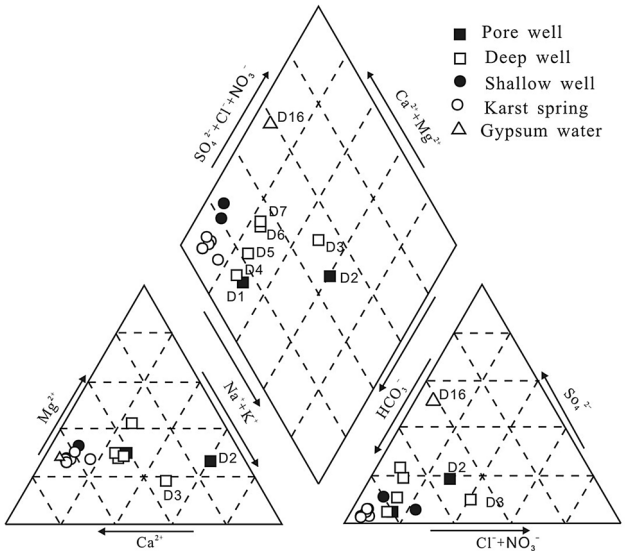

Fig. 2 Piper trilinear diagram of water samples

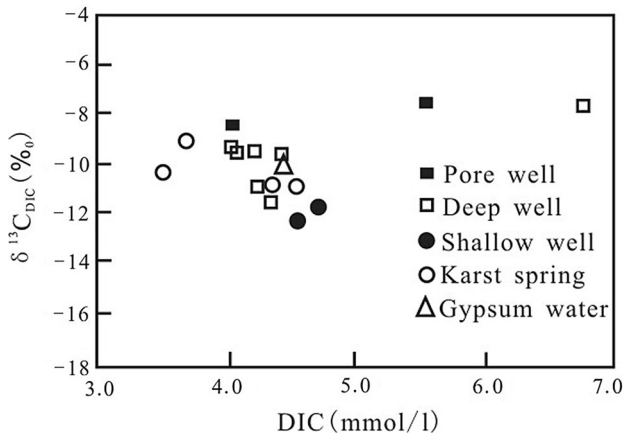

Fig. 3 DIC vs. $\delta^{13}C_{DIC}$ values in different types of groundwater

dissolution recorded the highest SO_4^{2-} concentration (5.62 mmol/L) among all the samples.

The piper trilinear diagram (Fig. 2) shows that, except for samples D2 and D3, Ca^{2+} and Mg^{2+} dominated the cation contents in these waters, which accounted for more than 71 % of the total cations in most groundwater samples. D2 and D3 in the southern covered karst region had a high Na^+ concentration of 5.61 and 3.16 mmol/L, respectively. Bicarbonate (HCO_3^-) was the dominant anion accounting for more than 60 % of TZ^- in all the samples, ranging from 3.53 to 6.74 mmol/L (Fig. 2). The second major anion was SO_4^{2-}, which ranged from 0.12 to 5.62 mmol/L. These values are much higher than those of karst groundwater in Guiling, southwest China, where the SO_4^{2-} only came from rainwater (Zhang et al. 2012). Chloride and nitrate concentrations ranged from 0.2 to 1.05 mmol/L (average 0.43 mmol/L) and from 0.07 to 0.90 mmol/L (average 0.21 mmol/L), respectively. Thus, except for samples D2 and D3, SO_4^{2-} and HCO_3^- together accounted for 78–94 % of the total anions.

Concentrations and carbon isotopes of DIC

When pH values range from 7.39 to 7.89, HCO_3^- was the dominant species of DIC and accounted for approximately 95 % of DIC (Li et al. 2010a, b). Therefore, the value of DIC was approximately equal to that of HCO_3^-. Concentrations of DIC were in the range of 3.53–6.74 mmol/L with a mean of 4.47 mmol/L (Table 1). These values are much higher than those of the groundwater in southeast China due to their slow speed of circulation and longer water–carbonate rock interaction time (Li et al. 2010a, b). In this study, there was no significant correlation between DIC and $\delta^{13}C_{DIC}$ (Fig. 3). The $\delta^{13}C$ values of DIC ranged from −12.25 to −7.53 ‰, with a mean value of −9.94 ‰ (Table 1), which was similar to the values in other regions. Cane and Clark (1999) revealed the similar conclusion when they studied $\delta^{13}C_{DIC}$ of groundwater in the areas with different land use. Chen et al. (2011) reported that Cambrian and Ordovician limestone and dolomite, which are present in the study area, have a $\delta^{13}C$ value of about +1.0 ‰, indicating that groundwater gets heavy carbon isotope from carbonate rock in the process of water circulation. In the study area, values of $\delta^{13}C_{DIC}$ in the groundwater of shallow wells and karst springs in northern bare karst area (−12.25 to −9.06 ‰) were generally lower than that of deep wells and quaternary pore water wells in the southern covered karst region (−9.59 to −7.53 ‰). Southern deep wells have a larger circulation depth and longer water–carbonate rock interaction time, resulting in more heavy carbon isotope from carbonate rock (Huang et al. 2012).

Sulfate (SO_4^{2-}) and S isotopes

The difference between $\delta^{34}S$ and SO_4^{2-} content is remarkable in different types of groundwater in the study area (Table 1). Figure 4 shows SO_4^{2-} has no significant correlation with $\delta^{34}S$, indicating that the groundwater of different types have different sulfate source. The values of $\delta^{34}S$ and SO_4^{2-} of gypsum mine water are the highest, with the value of 19.28 ‰ and 5.62 mmol/L, respectively. For the deep wells and quaternary pore water wells in the southern covered karst region, the $\delta^{34}S$ value were in the range of 8.73–19.35 ‰ and 9.46–11.05 ‰, respectively, and the SO_4^{2-} content ranged from 0.20 to 2.35 mmol/L and from 0.19 to 1.96 mmol/L, respectively. The values of $\delta^{34}S$ and SO_4^{2-} in the shallow wells and karst springs in northern bare karst area are the lowest, with the values of 4.53–6.42 ‰ and 0.12–0.62 mmol/L, respectively.

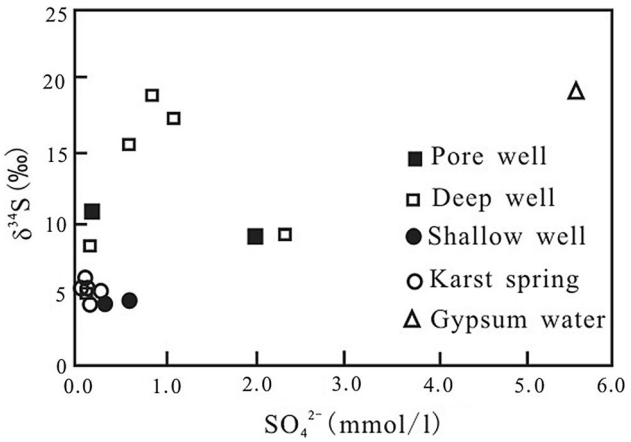

Fig. 4 SO_4^{2-} vs. $\delta^{34}S$ values in different types of groundwater

Discussion

Carbonate dissolution

The groundwater chemistry of karstic groundwater systems have been described thoroughly by Li et al. (2005) and Valdes et al. (2007). They have recognized that the karst hydrochemistry was controlled by the degree of dissolution of carbonate rocks with respect to pH conditions, temperature, local pCO_2, and other parameters. Saturation index of calcite ($SI_{calcite}$) and pCO_2 were computed using the data of Ca^{2+}, Mg^{2+}, alkalinity, pH and T measured in situ by the PHREEQC program (Version 2.15; Parkhurst and Appelo 1999).The covariations of pCO_2 and $\delta^{13}C_{DIC}$, and pCO_2 and $SI_{calcite}$, are shown in Fig. 5, respectively. No meaningful correlation between $\delta^{13}C_{DIC}$ and pCO_2 indicates that $\delta^{13}C_{DIC}$ value is controlled not only by pCO_2 but also by complex environmental factors (Clark and Fritz 1997). There is a negative correlation between $SI_{calcite}$ and pCO_2 ($R^2 = 0.33$, $n = 15$, $P < 0.001$), which means that the partial pressures of CO_2 control carbonate rock dissolution in the study area. All the groundwater was supersaturated due to their slow speed of circulation and longer water–carbonate rock interaction time (Table 1). In the study area, the aquifers were dominantly in carbonate rocks (limestone and dolomite), and therefore, the Ca·Mg–HCO_3 type chemistry of all the karst water samples is presumably the result of carbonate rock dissolution.

Sources of DIC

In natural karst groundwater, the equivalent ratio of $[Ca^{2+}+Mg^{2+}]/[HCO_3^-]$ is 1:1 in theory, (Yuan, 1997; Liu et al. 1997) if H_2CO_3 is derived only from carbonate dissolution by groundwater with soils pCO_2 [Eq. (1)]. For most of the karst groundwater in Fenyang, $Ca^{2+}+Mg^{2+}$ are largely in excess with respect to HCO_3^- (Fig. 6a), suggesting that additional acid was needed for carbonate rock dissolution. In the study area, the karst groundwater samples are rich in SO_4^{2-}. When $[SO_4^{2-}]$ is added to the denominator of $[Ca^{2+}+Mg^{2+}]/[HCO_3^-]$, the samples are scattered around the 1:1 line (Fig. 6b), suggesting that SO_4^{2-} obviously controls the electrovalent balance of anions in these studied water samples. Therefore, sulfuric acid might play a relatively important role in carbonate weathering in this study area. So, the main carbon sources to produce DIC in groundwater can originate from weathering of carbonate rocks by carbonic [Eq. (1)] and sulfuric acids [Eq. (2)] (Li et al. 2011):

$$Ca_{(1-x)}Mg_xCO_3 + CO_2 + H_2O = (1-x)Ca^{2+} + xMg^{2+} + 2HCO_3^- \quad (1)$$

$$2Ca_{(1-x)}Mg_xCO_3 + H_2SO_4 = 2(1-x)Ca^{2+} + 2xMg^{2+} + SO_4^{2-} + 2HCO_3^- \quad (2)$$

When DIC originate from weathering of carbonate rock by carbonic acid,the main carbon sources of DIC in groundwater will come from the carbonate rock and soil CO_2, in approximately equal amounts (Li et al. 2010a, b). The study area is dominated by C_3 plants, and $\delta^{13}C$ value of soil CO_2 is around −26 ‰ (Lu et al. 2012). Assuming carbonate rocks have a $\delta^{13}C$ value of about +1.0 ‰ in the study area (Chen et al. 2011), the $\delta^{13}C_{DIC}$ of the groundwater will approach to about −12.5 ‰ according to Eq. (1).

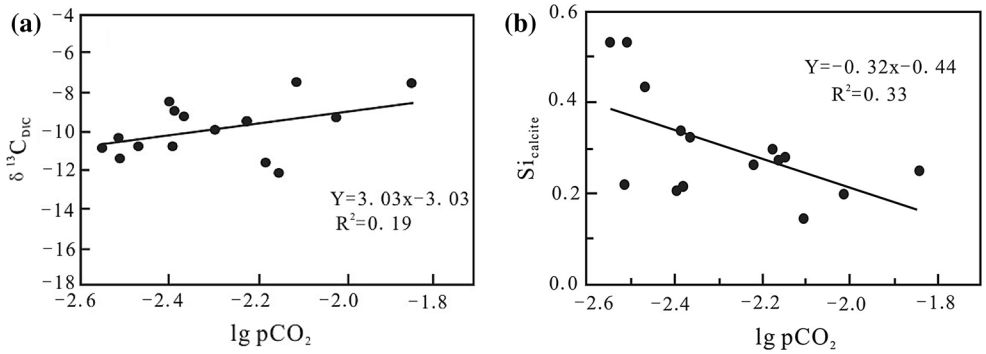

Fig. 5 The covariation of: **a** lg pCO2 vs. $\delta^{13}C_{DIC}$ and **b** lg pCO_2 vs. lg $SI_{calcite}$ in water samples

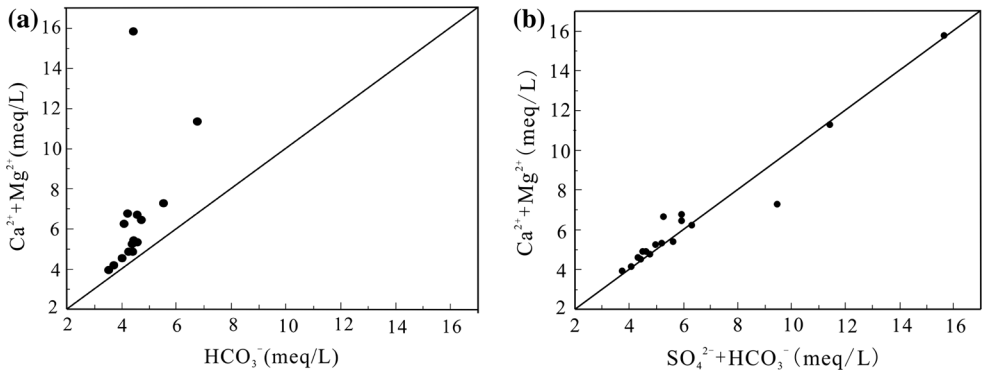

Fig. 6 The covariation of **a** $[Ca^{2+}+Mg^{2+}]$ vs. $[HCO_3^-]$; **b** $[Ca^{2+}+Mg^{2+}]$ vs.$[SO_4^{2-} + HCO_3^-]$ in water samples

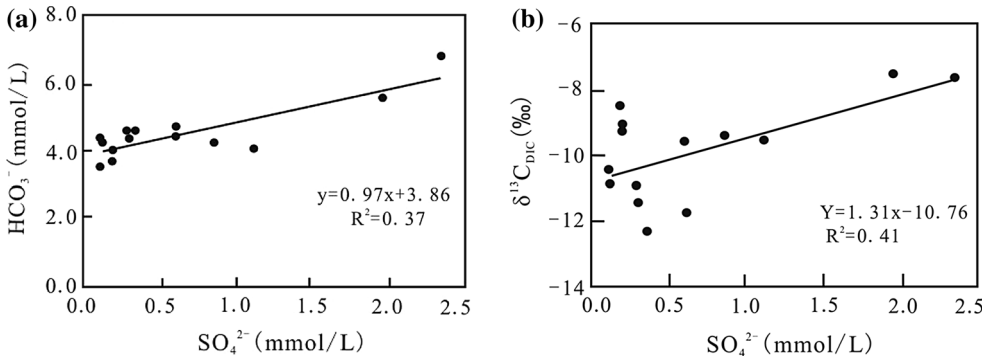

Fig. 7 The covariation of: **a** HCO_3^- vs. SO_4^{2-} and **b** $\delta^{13}C_{DIC}$ vs. SO_4^{2-} in water samples

However, if DIC comes from carbonate rock weathering by H_2SO_4 [Eq. (2)], the DIC will gain heavy $\delta^{13}C$ value (+1.0 ‰) from carbonate rocks. Therefore, the $\delta^{13}C_{DIC}$ values of the groundwater can be modified by sulfuric acid. The $\delta^{13}C$ values of DIC in the studied groundwater ranged from −12.25 to −7.53 ‰, with a mean value of −9.94 ‰, which is significantly greater than −12.5 ‰. Furthermore, there is a significantly positive correlation between SO_4^{2-} and HCO_3^- contents ($R^2 = 0.73$, $n = 15$, $P < 0.001$), and SO_4^{2-} and $\delta^{13}C_{DIC}$ value ($R^2 = 0.41$, $n = 15$, $P < 0.001$) of groundwater samples (Fig. 7a, b), which demonstrates that sulfuric acid dissolution of carbonate has important contribution to groundwater chemical composition and $\delta^{13}C_{DIC}$ value. Several studies have also shown that the sulfuric acid plays an important role in dissolution of carbonate in southwestern China (Han and Liu 2004; Xu and Liu 2007; Zhang et al. 2007; Yoon et al. 2008), Canadian Cordillera (Spence and Telmer 2005), the Ganges–Brahmaputra Basin (Galy and France-Lanord 1999) and Mackenzie Basin (Calmels et al. 2007).

Origin of sulfur

As shown in Fig. 5, no clear positive correlation was found between $\delta^{34}S$ and SO_4^{2-} equivalent ratio, implying that the sources of SO_4^{2-} are more complex. Dissolved SO_4^{2-} in groundwater can have different origins, mainly from dissolution of evaporite (gypsum), precipitation (atmospheric S deposition), oxidation of sulfide minerals in coal strata, and anthropogenic inputs (i.e., fertilizers, sewage, and mine drainage) (Li et al. 2010a, b).

The northern part of the study area around F3 fault is a bare karst area with limestone and dolomite of Cambrian and Ordovician age, while the southern part is a covered karst region, which is surrounded by F3, F4 and F5 faults, forming an enclosed karst water system (Fig. 1). There are no coal-bearing strata in bare karst area nor in covered karst region, which allows us to disregard sulfate contribution by sulfide oxidation. Several gypsum interbeds were contained in marl at the bottom of the upper and lower Ordovician Majiagou and Fengfeng formations (Duan and Liang 2006), so that the gypsum dissolution can increase SO_4^{2-} concentration in groundwater. Meanwhile, Shanxi province is one of major coal-producing provinces in China (Huai et al. 2011), which is impacted by serious sulfuric acid rain (Wang et al. 2000). Therefore, atmospheric acid deposition may also play a significant role in the increasing sulfate concentration in groundwater. In addition, the study area is located in the northern suburb of Fenyang City, just 5–10 km away from the town center. It is an important agricultural and industrial area with a large population. Therefore, sewage and industrial waste water can infiltrate through the upper loess layer and have adverse effects on the groundwater quality.

The SO_4^{2-} values of rainwater were 0.08–0.18 mmol/L from 2007 to 2011 (Li 2012) in Yuncheng City, which is 100 km away from Fenyang City. However, the differences of sulfate content and sulfur isotope composition are obvious among different potential sources (Table 2). Therefore, the values in Table 2 were used as the three end members in Fig. 8 to show how different types of groundwater are actually distributed. Except for samples D4 and D7, all the deep wells are located within the range of gypsum dissolution end member. It indicates that the SO_4^{2-} was mainly from gypsum dissolution with a larger circulation depth and longer water–carbonate rock interaction time. Sample D7 was located within the range of wastewater end member, indicating that the SO_4^{2-} mainly came from human contamination. Even though sample D7 is a deep well, it has not been pumped for a long time before sampled, and after having been pumped for a half-an-hour, the water color was still yellow. Therefore, the higher SO_4^{2-} content and low $\delta^{34}S$ value may come from mixing with the upper quaternary pore water. Sample D4 was collected from a main water supply well, which has a pump discharge of 1400 m^3 per day, leading to a quick cycle speed. This well is an important water source and much attention has been paid to protect its ecological environment. In this well the SO_4^{2-} influenced by gypsum dissolution and waste water was limited, and it was mainly from atmospheric precipitation.

The differences of geochemistry were obvious between samples D1 and D2 from quaternary pore water wells. The SO_4^{2-} content and $\delta^{34}S$ value of sample D1 were close to the range of atmospheric deposition end member, but sample D2 was located in waste water end member (Fig. 8). Sample D1 was near a farming area, with a single land use pattern and a relatively small population density. The influence from resident activities was limited, and the SO_4^{2-} was mainly from atmospheric precipitation. Sample D2 was near a staff living area of a large brewery factory and the well water was heavily used. The amount of industrial and municipal sewage is very large in this area to the dense population. Furthermore, wastewater can easily reach the quaternary aquifer system through surface soil, and would obviously impact the water quality. Meanwhile,

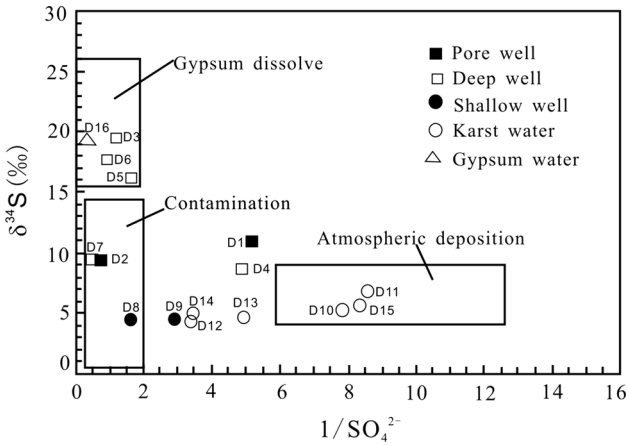

Fig. 8 $1/SO_4^{2-}$ (L/mmol)vs. $\delta^{34}S$ values in different types of groundwater

the Na^+ and Cl^- concentrations in sample D2 were also high, with values of 5.61 and 3.04 mmol/L, respectively, proving that the chemical components and the SO_4^{2-} were seriously affected by industrial and municipal wastewater.

The SO_4^{2-} content and $\delta^{34}S$ value of springs (D10, D11 and D15) were located in the range of atmospheric deposition end member, indicating that the SO_4^{2-} was mainly from rainwater. The three samples are from big karst springs with a discharge of more than 24.78 L/s (Table 1), with a quick water cycle speed and short water–carbonate rock interaction time, so that the SO_4^{2-} from gypsum dissolution is limited. Meanwhile, these springs are located in bare karst area with small population density, so that residential source of SO_4^{2-} is minimal. Other three karst springs (D13, D12, D14) were located in the mixed zone of wastewater and atmospheric precipitation (Fig. 8), implying that the SO_4^{2-} was derived from these two end members. These three karst springs have a small discharge (Table 1), and are the main water sources for villages, that have influence on the water chemical composition.

The SO_4^{2-} content and $\delta^{34}S$ value of the two shallow well samples (D8, D9) were mainly located in the range of wastewater end member. The two shallow wells are located in valley of the northern bare karst area and are used for drinking and irrigation.

Table 2 Sulfate contents and sulfur isotopic compositions of local potential sources

Type	SO_4^{2-} mmol/L	$\delta^{34}S$ ‰	Study area
Atmospheric deposition	0.08–0.18	4.88–9.34	Yuncheng city, Shanxi Province (Li 2012), the middle Yellow River (Hong et al. 1994)
contamination	0.5–3.0	0.6–14.5	Shuicheng basin, Guizhou province (Li et al. 2010), Chongqing (Li et al. 2006)
Gypsum water	0.51–18.37	15.85–25.65	Yangquan, Shanxi Province (Duan and Liang 2006), Niangziguang Spring Area, Shanxi Province (Li et al. 1998), Experimental Study (Raab and Spiro 1991)

Conclusions

The chemical composition of ground waters in Fenyang City were characterized by a dominance of Ca^{2+}, Mg^{2+}, HCO_3^- and SO_4^{2-}, which accounted for more than 85 % of the total ion concentrations. The carbonate rocks (limestone and dolomite) dissolution by weathering control groundwater chemical composition. The chemical and isotopic composition of groundwater is derived not only from carbonate dissolution by carbonic acid but also from sulfuric acid dissolution.

The low SO_4^{2-} content and $\delta^{34}S$ value of springs and shallow wells in north bare karst area were mainly from atmospheric deposition and human activities. The higher SO_4^{2-} content and low $\delta^{34}S$ value of quaternary pore water in the southern covered karst region mainly came from anthropogenic inputs, while the higher SO_4^{2-} content and $\delta^{34}S$ value of deep wells mainly came from dissolution of gypsum. The SO_4^{2+} of gypsum mine water was mainly from gypsum dissolution. The analytical results indicate that, comparing with the northern bare karst area, human activities have significantly changed the groundwater chemical composition in the southern covered karst region. Therefore, more measures should be taken on the groundwater protection in the southern covered karst region in the future.

Acknowledgments This work was financially supported by the National Natural Science Foundation of China (No: 41302211), the Special Fund for Public Benefit Scientific Research of Ministry of Land and Resources of China (No: 12120113005200). Special thanks are given to the prof. Liang Yongping for his valuable comments and suggestions. Thanks are also given to Mr. Zhao Shiyong and Wang Weitang for their help in the field.

References

Atekwana EA, Krishnamurthy RV (1998) Seasonal variations of dissolved inorganic carbon and $\delta^{13}C$ of surface water: application of a modified gas evolution technique. J Hydrol 205:265–278

Beynen P, Feliciano N, North L, Townsend K (2007) Application of a karst disturbance index in Hillsborough County, Florida. Environ Manag 39(2):261–277

Bottrell S, Tellam J, Bartlett R, Hughes A (2008) Isotopic composition of sulfate as a tracer of natural and anthropogenic influences on groundwater geochemistry in an urban sandstone aquifer, Birmingham, UK. Appl Geochem 23(8):2382–2394

Calmels D, Gaillardet J, Brenot A, France-Lanord C (2007) Sustained sulfide oxidation by physical erosion processes in the Mackenzie River basin: climatic perspectives. Geology 35:1003–1006

Cane G, Clark ID (1999) Tracing ground water recharge in an agricultural watershed with isotopes. Ground Water 37:133–139

Chen JT, Chough SK, Han ZZ, Lee JH (2011) An extensive erosion surface of a strongly deformed limestone bed in the Gushan and Chaomidian formations (late Middle Cambrian to Furongian), Shandong Province, China: sequence–stratigraphic implications. Sed Geol 233(1–4):129–149

Clark ID, Fritz P (1997) Environmental Isotopes in Hydrogeology. Lewis Publishers, New York

Duan GW, Liang YP (2006) The use of $\delta^{34}S$ in the analysis of sulfate contamination on karst groundwater in Yangquan. West-China Exp Eng 18(1):100–103 **(in Chinese with English abstract)**

Fan YH, Huo XL, Hao YH, Liu Y, Wang TK, Liu YC, Yeh TJ (2013) An assembled extreme value statistical model of karst spring discharge. J Hydrol 504:57–68

Galy A, France-Lanord C (1999) Weathering processes in the Ganges–Brahmaputra basin and the riverine alkalinity budget. Chem Geol 159:31–60

Gams I, Nicod J, Julian M, Anthory E, Sauro U (1993) Environmental change and human impacts on the Mediterranean karsts of France, Italy and the Dinaric Region. In: Williams PW (ed) Karst terrians: environmental changes, human impact: catena supplement 25. Catena Verlag, Cremlingen-Destedt, Germany

Guo Q, Wang Y, Ma T, Li L (2005) Variation of karst springs discharge in recent five decades as an indicator of global climate change: a case study at Shanxi, northern China. Sci China Series D Earth Sci 48(11):2001–2010

Han GL, Liu CQ (2004) Water geochemistry controlled by carbonate dissolution: a study of the river waters draining karst-dominated terrain, Guizhou Province, China. Chem Geol 204:1–21

Han DM, Xu HL, Liang X (2006) GIS-based regionalization of a karst water system in Xishan Mountain area of Taiyuan Basin, north China. J Hydrol 331:459–470

Heinz B, Birk S, Liedl R, Geyer T, Straub KL, Andresen J, Bester K, Kappler A (2008) Water quality deterioration at a karst spring (Gallusquelle, Germany) dueto combined sewer overflow: evidence of bacterial and micro-pollutant contamination. Environ Geol 57(4):797–801

Hong YT, Zhang HH, Zhu YX, Pu HC, Jiang HB, Liu DP (1994) Characteristics of sulfur isotopic composition of meteoric water in China. Prog Nat Sci 4(6):741–745 **(in Chinese with English abstract)**

Hosono T, Wang C, UmezawaY Nakano T, Onodera S, Nagata T, Yoshimizu C, Tayasu I, Taniguchi M (2010) Multiple isotope (H, O, N, S and Sr) approach elucidates complex pollution causes in the shallow groundwaters of the Taipei urban area. J Hydrol 397(1–2):23–36

Huai HY, Gaines A, Tye RE (2011) Relation between the deposition and petrology of Shanxi coals and the composition of their extracts. Appl Geochem 26(8):1377–1385

Huang QB, Qin XQ, Liu PY (2012) The $\delta^{13}C$ characteristics of groundwater in different karst environmental conditions. Earth and Environment 40(4):505–511 **(in Chinese with English abstract)**

Jemcov I (2007) Water supply potential and optimal exploitation capacity of karst aquifer systems. Environ Geol 51(5):767–773

Krouse HR, Mayer B (2000) Sulphur and oxygen isotopes in sulphate. In: Cook PG, Herczeg AL (eds) Environmental Tracers in Subsurface Hydrology. Kluwer Academic Press, Boston

Lang YC, Liu CQ, Li SL, Zhao ZQ, Zhou ZH (2011) Tracing natural and anthropogenic sources of dissolved sulfate in a karst region by using major ion chemistry and stable sulfur isotopes. Applied Geochemistry 26:S202–S205

Li YP (2012) The analysis on characteristics and trend of precipitation in Yuncheng City. Sci Technol Enterp 3(9):154–155 **(in Chinese with English abstract)**

Li YL, Wang YX, Liu J, Lou ZH (1998) Pollution analysis of SO_4^{2-}, Ca^{2+}, Mg^{2+} in karst water in Niang Ziguan Spring area. Geol Sci Technol Inform 17(2):111–114 **(in Chinese with English abstract)**

Li SL, Liu CQ, Tao FX, Lang YC, Han GL (2005) Carbon biogeochemistry of ground water, Guiyang, Southwest China. Ground Water 43:494–499

Li XD, Masuda H, Kusakabe M, Yanagisawa F, Zeng HA (2006) Degradation of groundwater quality due to anthropogenic sulfur and nitrogen contamination in the Sichuan Basin, China. Geochem J 40(4):309–332

Li SL, Calmels D, Han GL, Gaillardet J, Liu CQ (2008) Sulfuric acid as an agent of carbonate weathering constrained by $\delta^{13}C_{DIC}$: examples from Southwest China. Earth Planet Sci Lett 270:180–199

Li SL, Liu CQ, Li J, Lang YC, Ding H, Li LB (2010a) Geochemistry of dissolved inorganic carbon and carbonate weathering in a small typical karstic catchment of Southwest China: isotopic and chemical constraints. Chem Geol 277:301–309

Li XD, Liu CQ, Harue M, Li SL, Liu XL (2010b) The use of environmental isotopic (C, Sr, S) and hydrochemical tracers tocharacterize anthropogenic effects on karst groundwater quality: a case study of the Shuicheng Basin, SW China. Appl Geochem 25:1924–1936

Li XD, Liu CQ, Liu XL, LiR Bao (2011) Identification of dissolved sulfate sources and the role of sulfuric acid in carbonate weathering using dual-isotopic data from the Jialing River, Southwest China. J Asian Earth Sci 42:370–380

Liang YP, Wang WT, Zhao CH, Wang W, Tang CL (2013) Variations of karst water and environmental problems in North China. Carsologica Sinica 32(1):34–42 **(in Chinese with English abstract)**

Liu ZH, Yuan DX, He SY (1997) Stable Carbon Isotope Geochemical and Hydrochemical Features in the System of Carbonate–H_2O–CO_2 and Their Implications-Evidence from Several Typical Karst Area of China. Acta Geologica Sinica (English Edition) 71(4):446–454

Liu CQ, Lang YC, Satake H, Wu JH, Li SL (2008) Identification of anthropogenic and natural inputs of sulfate and chloride into the karstic ground water of Guiyang, SW China: combined $\delta^{37}Cl$ and $\delta^{34}S$ approach. Environ Sci Technol 429(15):5421–5427

Lu HY, ZhouYL Liu WG, Mason J (2012) Organic stable carbon isotopic composition reveals late Quaternary vegetation changes in the dune fields of northern China. Quatern Res 77(3):433–444

Otero N, Canals À, Soler A (2007) Using dual-isotope data to trace the origin and processes of dissolved sulphate: a case study in Calders stream (Llobregat basin, Spain). Aquat Geochem 13:109–126

Parkhurst DL, Appelo CAJ (1999) User's Guide to PHREEQC (Version 2)-A Computer Program for Speciation, Batch-reaction, One-dimensional Transport, and Inverse Geochemical Calculations. US Geol Surv Water-Resour Invest Rep 99–4259

Raab M, Spiro B (1991) Sulfur isotopic variations during seawater evaporation with fractional crystallization. Chem Geol 86(4):323–333

Sauro U (1993) Human impact on the karst of the Venetian Fore-Alps. Italy. Environmental Geology 21(3):115–121

Spence J, Telmer K (2005) The role of sulfur in chemical weathering and atmospheric CO_2 fluxes: evidence from major ions, $\delta^{13}C_{DIC}$, and$\delta^{34}S_{SO4}$ in rivers of the Canadian Cordillera. Geochim Cosmochim Acta 69:5441–5458

Valdes D, Dupont JP, Laignel B, Oiger S, Leboulanger T, Mahler BJ (2007) A spatial analysis of structural controls on karsts groundwater geochemistry at a regional scale. J Hydrol 340:244–255

Wang TJ, Jin LS, Lia ZK, Lam KS (2000) A modeling study on acid rain and recommended emission control strategies in China. Atmos Environ 34(26):4467–4477

Wang YX, Guo QH, Su CL, Ma T (2006) Strontium isotope characterization and major ion geochemistry of karst water flow, Shentou, northern China. J Hydrol 328:592–603

Xu ZF, Liu CQ (2007) Chemical weathering in the upper reaches of Xijiang River draining the Yunnan-Guizhou Plateau. Southwest China. Chem. Geol 239:83–95

Yanagisawa F, Sakai H (1983) Thermal decomposition of barium sulfate-vanadium pentoxide-silica glass mixtures for preparation of sulfur dioxide in sulfur isotope ratio measurements. Anal Chem 55(6):985–987

Yang YC, Shen ZL,Wen DG, Hou GC, She HQ, Zhao ZH, Wang D, Li JW (2010) Distribution of $\delta^{34}S$ and $\delta^{18}O$ in SO_4^{2-} in groundwater from the ordos cretaceous groundwater baisn and geological implications. Acta Geologica Sinica (English Edition) 84(2):432–440

Yoon J, Huh Y, Lee I, Moon S, Noh H, Qin JH (2008) Weathering processes in the Min Jiang: major elements, $^{87}Sr/^{86}Sr$, $\delta^{34}S_{SO4}$, and$\delta^{18}O_{SO4}$. Aquat Geochem 14:147–170

Yuan DX (1997) Sensitivity of karst process to environmental change along the PEP II transect. Quatern Int 35:105–113

Zhang SR, Lu XX, Higgitt DL, Chen CTA, Sun HG, Han JT (2007) Water chemistry of the Zhujiang (Pearl River): natural processes and anthropogenic influences. J Geophys Res 112:F01011. doi:10.1029/2006JF000493

Zhang JH, Liang YP, Wang WT, Han XR, Hou GC (2009) A practical use of $\delta^{34}S$ in the investigation of karst groundwater resource in North China. Carsologica Sinica 28(3):235–241 **(in Chinese with English abstract)**

Zhang HB, Yu S, He SY, Liu Q, Li YL (2012) Analysis on the chemical characteristics of the atmospheric precipitation in Guilin. Carsologica Sinica 31(3):289–295 **(in Chinese with English abstract)**